

Clustering of Rapidly Settling, Low-Inertia Particle Pairs in Isotropic Turbulence.

II. Comparison of Theory and DNS

SARMA L. RANI^{1†}, ROHIT DHARIWAL², and
DONALD L. KOCH³

¹Department of Mechanical and Aerospace Engineering, University of Alabama in Huntsville, Huntsville, Alabama 35899, U.S.A.

²Department of Civil and Environmental Engineering, Duke University, Durham, North Carolina 27708, U.S.A.

³School of Chemical and Biomolecular Engineering, Cornell University, Ithaca, New York 14853, U.S.A.

(Received xx; revised xx; accepted xx)

Part I of this study presented a stochastic theory for the clustering of monodisperse, rapidly settling, low-Stokes-number particle pairs in homogeneous isotropic turbulence. The theory involved the development of closure approximations for the drift and diffusion fluxes in the probability density function (PDF) equation for pair relative positions. In this Part II paper, the theory is quantitatively analyzed by comparing its predictions of particle clustering with data from direct numerical simulations (DNS) of isotropic turbulence containing particles settling under gravity. DNS were performed at a Taylor micro-scale Reynolds number $Re_\lambda = 77.76$ for three Froude numbers $Fr = \infty, 0.052, 0.006$. The Froude number Fr is defined as the ratio of the Kolmogorov scale of acceleration and the magnitude of gravitational acceleration. Thus, $Fr = \infty$ corresponds to zero gravity, and $Fr = 0.006$ to the highest magnitude of gravity among the three DNS cases. For each Fr , particles of six Stokes numbers in the range $0.01 \leq St_\eta \leq 0.2$ were tracked in the DNS, and particle clustering quantified both as a function of separation and the spherical polar angle. We compared the DNS and theory values for the power-law exponent β characterizing the dependence of clustering on separation. Reasonable agreement is seen between the DNS β 's for the $Fr = 0.006$ case and the theoretical predictions obtained using the second drift closure (referred to as DF2). Further, in conformity with the DNS, theory shows that the clustering of $St_\eta \ll 1$ particles is only weakly anisotropic.

1. Introduction

This paper presents the Part II of the current work on a stochastic theory for the clustering of monodisperse, low-inertia particle pairs that are settling rapidly in homogeneous isotropic turbulence. The theory is developed in the limits of $Fr \ll St_\eta \ll 1$, where the Stokes number St_η is the ratio of the particle response time to the Kolmogorov time scale. The Part I paper presented the derivation of: (1) closure approximations for the drift and diffusion fluxes in the probability density function (PDF) equation for pair relative positions, and (2) the analytical solution to the PDF $\langle P \rangle(r, \theta)$, where r is the separation, and θ is the spherical polar angle. Part II focuses on the quantitative analysis of the theory by comparing its predictions of particle clustering with the results from DNS of isotropic turbulence containing particles settling under gravity.

† Email address for correspondence: sarma.rani@uah.edu

Gravitational settling modifies particle dynamics in important ways. One of the main effects of gravity is that it introduces anisotropy into the particle sampling of the underlying turbulence, and thereby in the spatial clustering of particles. Gravity also alters the correlation times of fluid velocity gradients along particle trajectories. The altered time scales, in turn, modulate the path-history effects that play a key role in determining particle clustering (Part I paper presents a more detailed discussion of the path-history effects and their role in clustering). The theory developed in this study incorporates the effects on clustering of settling-induced anisotropy, as well as of settling-modulated flow time scales.

Recently, Ireland *et al.* (2016) performed a detailed DNS investigation of the effects of gravity on the dynamics of single particles, as well as particle pairs. In their study, the Froude number $Fr = 0.052$, which is representative of fluid accelerations in cumulus clouds. They considered a wide range of Taylor micro-scale Reynolds numbers ($88 \leq Re_\lambda \leq 597$), Stokes numbers ($0 \leq St_\eta \leq 56.2$). For $St_\eta < 1$, they showed that the principal effect of gravity on particle clustering was to decrease the inward (radial) drift, thereby reducing the radial distribution function (RDF). They also found that gravity mitigates the preferential concentration mechanism by reducing the interaction time between particles and the underlying turbulence. Specifically, gravity reduces the Lagrangian time scales of strain-rate and rotation-rate along particle trajectories. As shown in Chun *et al.* (2005), the drift flux is proportional to the time integral of the two-time correlation of $[S^2(t) - R^2(t)]$ along the trajectory of the primary particle, where S^2 and R^2 are the second invariants of the strain-rate and rotation-rate tensors, respectively. Ireland *et al.* (2016) also quantified the anisotropy in particle clustering due to gravity through the use of spherical harmonic functions to represent the RDF dependence on the polar angle θ .

Bec *et al.* (2014) performed a DNS study of the effects of settling on inertial particle clustering in isotropic turbulence. They considered both low and high Stokes number particles ($St_\eta \lesssim 1$ and $St_\eta > 1$, respectively) that are settling under low- and high-gravity conditions ($Fr > 1$ and $Fr < 1$, respectively). Bec *et al.* (2014) observed that when $Fr \ll 1$, the clustering of $St_\eta \lesssim 1$ particles decreased and became anisotropic in that particles formed streaks along the vertical (or gravity) direction. The opposite effect is seen for $St_\eta > 1$ particles, whose clustering increased when compared to the zero-gravity case. The opposing effects of gravity on the clustering of low- and high-Stokes number particles was also seen by Ireland *et al.* (2016). Other DNS studies of settling particles (Ayala *et al.* 2008; Onishi *et al.* 2009; Woittiez *et al.* 2009; Parishani *et al.* 2015) focused primarily on the collision rates of droplets in isotropic turbulence.

In this Part II paper, we present a comparison of the theory-predicted particle clustering with the corresponding DNS data. For Stokes numbers $St_\eta \ll 1$, we compare the exponent β characterizing the power-law dependence of the PDF $\langle P \rangle(r, \theta)$ on separation r . We also compare the degree of anisotropy of clustering obtained from the theory with that from DNS. In the case of DNS, particle clustering is quantified at $Re_\lambda = 77.76$ for three Froude numbers $Fr = \infty, 0.052, 0.006$ (in the order of increasing gravity), and six Stokes numbers in the range $0.01 \leq St_\eta \leq 0.2$. For the highest gravity case, $Fr = 0.006$, the particle settling time through the periodic box of length 2π is close to the integral time scale. This may lead to errors since particles that have exited the domain and been reintroduced into it will again encounter the same correlated eddies that they have already seen previously on their way down the box (Ireland *et al.* 2016; Woittiez *et al.* 2009). To eliminate this numerical artifact, we performed DNS with a bigger domain size of 4π along the vertical direction for the $Fr = 0.006$ case.

The organization of the paper is as follows. Section 2 presents the computational

details of the DNS runs, as well as the particle evolution algorithm. Quantification of the two-time correlations of dissipation rate and enstrophy is discussed in Section 3. The development of model energy spectrum that closely matches the DNS energy spectrum is presented in Section 4. In section 5, we present the comparison of theory predictions of particle clustering with the DNS data. Section 6 summarizes the key findings of this Part II paper.

2. Computational Method

2.1. Fluid Phase

Direct numerical simulations of forced isotropic turbulence were performed using a pseudo-spectral method based on the discrete Fourier expansions of flow variables. The simulation domain, consisting of a cube of length 2π , is discretized into N^3 grid points, with periodic boundary conditions along the three cartesian directions.

The governing equations for the flow are the Navier-Stokes equations in rotational form and the continuity equation (Ireland *et al.* 2013; Brucker *et al.* 2007)

$$\frac{\partial \mathbf{u}}{\partial t} + \boldsymbol{\omega} \times \mathbf{u} = -\nabla (p/\rho_f + \mathbf{u}^2/2) + \nu \nabla^2 \mathbf{u} \quad (2.1)$$

$$\nabla \cdot \mathbf{u} = 0 \quad (2.2)$$

where $\boldsymbol{\omega} = \nabla \times \mathbf{u}$ is the vorticity, ρ_f is the fluid density, and p is the pressure.

Transforming Eqs. (2.1) and (2.2) into Fourier space and eliminating pressure using the spectral form of continuity yields

$$\left(\frac{\partial}{\partial t} + \nu k^2 \right) \hat{\mathbf{u}} = - \left(\mathbf{I} - \frac{\mathbf{k}\mathbf{k}}{k^2} \right) \cdot \widehat{\boldsymbol{\omega} \times \mathbf{u}} \quad (2.3)$$

where $k^2 = \mathbf{k} \cdot \mathbf{k}$. Direct evaluation of the convolution $\widehat{\boldsymbol{\omega} \times \mathbf{u}}$ is extremely computationally intensive. Hence, a pseudo-spectral approach is adopted wherein $\boldsymbol{\omega} \times \mathbf{u}$ is first computed in physical space, and then transformed into the spectral space.

Since the time-derivative and viscous stress terms on the LHS of Eq. (2.3) are linear in $\hat{\mathbf{u}}$, one may evolve these terms in time exactly by multiplying Eq. (2.3) with the integrating factor, $\exp(\nu k^2 t)$. This yields the following equation (in index notation):

$$\frac{\partial}{\partial t} [\exp(\nu k^2 t) \hat{u}_i] = \text{RHS}_i \exp(\nu k^2 t), \quad (2.4)$$

where $\text{RHS}_i = (-\delta_{im} + \frac{k_i k_m}{k^2}) \epsilon_{mjk} \mathcal{F}\{\omega_j u_k\}$ represents the right-hand side of Eq. (2.3), and $\epsilon_{mjk} \mathcal{F}\{\omega_j u_k\}$ represents the convolution $\widehat{\boldsymbol{\omega} \times \mathbf{u}}$, and ϵ_{mjk} is the Levi-Civita tensor.

Equation (2.4) is then discretized in time using the second-order Runge-Kutta (RK2) method giving

$$\hat{u}_i^{n+1} = \hat{u}_i^n \exp(-\nu k^2 t) + \{\text{RHS}_i^n \exp(-\nu k^2 t) + \text{RHS}_i^{n+1}\} \quad (2.5)$$

where n is the previous time-step level and h is the time-step size. To prevent convective instabilities, time-step size h is chosen such that the CFL number ≤ 0.5 . The pseudospectral algorithm introduces aliasing errors which are removed by zeroing the fluid velocities in spectral space for wavenumbers satisfying $k \geq k_{\max}$, where k is the wavenumber magnitude, $k_{\max} = \sqrt{2}N/3$, and N is the number of grid points along each dimension.

To achieve statistically stationary turbulence, we employ the deterministic forcing method developed by Witkowska *et al.* (1997), wherein the turbulent kinetic energy

dissipated during a time step is added back to the flow at the low wavenumbers. It may be noted that in this method, there is no explicit forcing term \mathbf{f} added to the Navier-Stokes equations. Instead, one scales the velocity components in the wavenumber band $[\kappa_{\min}, \kappa_{\max}]$ by a factor such that the energy dissipated during a given time step is resupplied, as follows.

$$\hat{\mathbf{u}}(\boldsymbol{\kappa}, t + \Delta t) = \hat{\mathbf{u}}(\boldsymbol{\kappa}, t + \Delta t) \sqrt{1 + \frac{\Delta E_{\text{diss}}(\Delta t)}{\int_{\kappa_{\min}}^{\kappa_{\max}} E(\boldsymbol{\kappa}, t + \Delta t) d\boldsymbol{\kappa}}} \quad \forall \boldsymbol{\kappa} \in [\kappa_{\min}, \kappa_{\max}] \quad (2.6)$$

where $\hat{\mathbf{u}}(\boldsymbol{\kappa}, t)$ is the spectral velocity, ΔE_{diss} is the total energy dissipated during Δt , and $E(\boldsymbol{\kappa}, t + \Delta t)$ is the spectral turbulent kinetic energy in a wavenumber shell with magnitude $\boldsymbol{\kappa}$ at time $t + \Delta t$. In the current study, the velocity components in the range $\boldsymbol{\kappa} \in (0, \sqrt{2}]$ are forced using Eq. (2.6).

2.2. Particle Phase

The governing equations of motion for a heavy spherical particle, whose diameter is much smaller than the Kolmogorov length scale, may be written as

$$\frac{d\mathbf{x}_p}{dt} = \mathbf{v}_p, \quad (2.7)$$

$$\frac{d\mathbf{v}_p}{dt} = \frac{\mathbf{u}(\mathbf{x}_p, t) - \mathbf{v}_p}{\tau_v} + \mathbf{g}, \quad (2.8)$$

where we assumed Stokes drag to be the principal force on the particle, \mathbf{x}_p and \mathbf{v}_p are the particle position and velocity, respectively, and τ_v is the particle viscous relaxation time. In Eq. (2.8), $\mathbf{u}(\mathbf{x}_p, t)$ is the fluid velocity at the particle's location. We neglect two-way coupling effects, as well as particle collisions. In order to solve Eqs. (2.7) and (2.8) numerically, $\mathbf{u}(\mathbf{x}_p, t)$ needs to be evaluated. This is achieved by interpolating, to the particle position, fluid velocities at a stencil of grid points surrounding the particle. We use the 8th order Lagrange interpolation method that is based on a stencil of $8 \times 8 \times 8$ fluid velocities.

Temporal update of particle motion is achieved through a modified second-order Runge-Kutta (RK2) method in which the standard RK2 weights are replaced by exponential integrators as follows Ireland *et al.* (2013).

$$\mathbf{v}_p(t_0 + h) = e^{-h/\tau_v} \mathbf{v}_p(t_0) + w_1 \mathbf{u}[\mathbf{x}_p(t_0)] + w_2 \mathbf{u}[\mathbf{x}_p(t_0) + \mathbf{v}_p(t_0)h] + (1 - e^{-h/\tau_v})\tau_v \mathbf{g}, \quad (2.9)$$

where h is the time step, and the exponential integrators w_1 and w_2 are given by

$$w_1 \equiv \left(\frac{h}{\tau_v}\right) \left[\phi_1\left(\frac{-h}{\tau_v}\right) - \phi_2\left(\frac{-h}{\tau_v}\right) \right], \quad w_2 \equiv \left(\frac{h}{\tau_v}\right) \phi_1\left(\frac{-h}{\tau_v}\right) \quad (2.10)$$

$$\phi_1(z) \equiv \frac{e^z - 1}{z}, \quad \phi_2(z) \equiv \frac{e^z - z - 1}{z^2} \quad (2.11)$$

For small values of Fr , the periodic box length L is an important consideration since it can artificially influence the motion of settling, inertial particles. Specifically, the use of periodic boundary conditions is problematic if the time it takes the settling particles to traverse the length L is $\leq O(T_E)$, where T_E is the large eddy turnover time. Several studies (Woittiez *et al.* 2009; Ireland *et al.* 2016; Dhariwal & Bragg 2018) considered this issue in detail and found that box sizes larger than $L = 2\pi$ may be needed, particularly when $St_\eta \gtrsim 1$. In this paper, the smallest Froude number is $Fr = 0.006$. Considering $St_\eta = 0.1$, $Fr = 0.006$, and $T_E = 1.568$, it can be shown that the settling times of particles through a domain length $L = 2\pi$ is $T_{\text{settle}}^{L=2\pi} \approx 1.75$. Since $T_{\text{settle}}^{L=2\pi}$ is only marginally

greater than T_E , we considered a box dimension of 4π along the direction of gravity for the $Fr = 0.006$ case.

3. Correlation Times in Second Drift Closure: $T_{\epsilon\epsilon}$, $T_{\zeta\zeta}$, $T_{\epsilon\zeta}$, $T_{\zeta\epsilon}$

The drift flux $q_i^d(\mathbf{r}, t)$ in the transport equation for the PDF $\langle P \rangle$ is given by

$$q_i^d(\mathbf{r}, t) = -\langle P \rangle(\mathbf{r}; t) \frac{St_\eta^2}{T_\eta^2} r_k \int_{-\infty}^t d_{ik} dt' \quad (3.1)$$

where T_η is the inverse of the Kolmogorov time scale. In the Part I paper, we derived two closure forms for the integral on the right-hand side (RHS) of (3.1), referred to as DF1 and DF2. DF1 is based on the assumption that the fluid velocity gradient along particle trajectories has a Gaussian distribution. In DF2, we regard the strain-rate and rotation-rate tensors scaled by the turbulent dissipation rate and enstrophy, respectively, as normally distributed.

In the second closure of drift flux (DF2), this integral is given by

$$\begin{aligned} \int_{-\infty}^t d_{ik} dt' = & \frac{1}{4\nu^2} \left\{ \frac{1}{3} \delta_{ik} [\langle \epsilon^2 \rangle T_{\epsilon\epsilon} + \langle \epsilon \zeta \rangle T_{\epsilon\zeta} - \langle \zeta \epsilon \rangle T_{\zeta\epsilon} - \langle \zeta^2 \rangle T_{\zeta\zeta}] + \right. \\ & 2\langle \epsilon^2 \rangle \int_{-\infty}^t \exp\left(-\frac{t-t'}{T_{\epsilon\epsilon}}\right) \langle \sigma_{ij}(t) \sigma_{lm}(t') \rangle \langle \sigma_{jk}(t) \sigma_{lm}(t') \rangle dt' - \\ & \left. 2\langle \zeta^2 \rangle \int_{-\infty}^t \exp\left(-\frac{t-t'}{T_{\zeta\zeta}}\right) \langle \rho_{ij}(t) \rho_{lm}(t') \rangle \langle \rho_{jk}(t) \rho_{lm}(t') \rangle dt' \right\}. \end{aligned} \quad (3.2)$$

Equation (3.2) contains the auto- and cross-correlation times of the dissipation rate ϵ and enstrophy ζ — $T_{\epsilon\epsilon}$, $T_{\zeta\zeta}$, $T_{\epsilon\zeta}$, and $T_{\zeta\epsilon}$. These are approximated to be along the trajectories of fluid particles collocated with the inertial particles. Furthermore, since the particles are settling rapidly ($St_\eta = g\tau_v/u_\eta \gg 1$), we may regard the surrounding turbulence as essentially frozen during a particle response time τ_v . Therefore, based on the Taylor's hypothesis, the Lagrangian time scales may be expressed as the respective spatial correlation lengths divided by the particle settling velocity. For instance, $T_{\epsilon\epsilon} = L_{\epsilon\epsilon}/g\tau_v$, and $T_{\epsilon\zeta} = L_{\epsilon\zeta}/g\tau_v$. Due to isotropy, $L_{\epsilon\zeta} = L_{\zeta\epsilon}$, so that the terms $\langle \epsilon \zeta \rangle T_{\epsilon\zeta}$ and $(-\langle \zeta \epsilon \rangle T_{\zeta\epsilon})$ cancel out on the RHS of (3.2). Therefore, the unknown length scales are $L_{\epsilon\epsilon}$ and $L_{\zeta\zeta}$. We now discuss the procedure for computing the length scale $L_{\epsilon\epsilon}$ through DNS (an analogous process is used to compute $L_{\zeta\zeta}$).

The length scale $L_{\epsilon\epsilon}$ is defined as

$$L_{\epsilon\epsilon} = \frac{\int R_{\epsilon\epsilon}(r) dr}{\langle \epsilon^2 \rangle} \quad (3.3)$$

where $R_{\epsilon\epsilon}(r) = \langle \epsilon(\mathbf{x}; t) \epsilon(\mathbf{x} + \mathbf{r}; t) \rangle$ is the spatial correlation of dissipation rate. It is evaluated using Fourier transforms as

$$R_{\epsilon\epsilon}(r) = \int d\boldsymbol{\kappa} \Phi_{\epsilon\epsilon}(\boldsymbol{\kappa}) e^{i\boldsymbol{\kappa} \cdot \mathbf{r}} \quad (3.4)$$

where $\Phi_{\epsilon\epsilon}$ is the Fourier coefficient of $R_{\epsilon\epsilon}$, and $\boldsymbol{\kappa}$ and \mathbf{r} are the wavenumber and relative position vectors, respectively. Expressing the integral $\int d\boldsymbol{\kappa}$ in spherical coordinates, and performing the integrations in polar and azimuthal angles, we have

$$R_{\epsilon\epsilon}(r) = \int d\kappa D_\epsilon(\kappa) \frac{\sin(\kappa r)}{\kappa r} \quad (3.5)$$

| $L_{\epsilon\epsilon}$ | $L_{\zeta\zeta}$ |
|------------------------|------------------|
| 0.257 | 0.211 |

Table 1: Correlation length scales of ϵ and ζ for $Re_\lambda = 77.76$.

where $\kappa = |\boldsymbol{\kappa}|$ and

$$D_\epsilon(\kappa) = \left\langle \sum_{|\boldsymbol{\kappa}|=\kappa} \widehat{\epsilon}(\boldsymbol{\kappa}, t) \widehat{\epsilon}^*(\boldsymbol{\kappa}, t) \right\rangle \quad (3.6)$$

In the above equation, $\widehat{(\cdot)}$ denotes the Fourier coefficient, and the superscript $*$ the complex conjugate. We evaluate $D_\epsilon(\kappa)$ using DNS, while the integral in (3.5) is calculated through numerical quadrature. In (3.6), $\langle \cdots \rangle$ denotes averaging over an ensemble of temporal snapshots of the statistically stationary turbulent velocity field. The length scales thus determined from the current DNS are given in Table 1.

4. DNS Inputs to Theory

To be able to consistently compare theory and DNS, it is important that the theory use the same turbulence parameters as those in statistically stationary DNS. Hence, inputs to the theory such as the Kolmogorov and integral length scales, dissipation rate, kinematic viscosity, root-mean-square velocity u_{rms} , and Re_λ are all identical to those in Table 2, which lists the DNS turbulence parameters. In particular, one also has to ensure that the energy spectrum $E(\kappa)$ needed in the theory (to compute the drift and diffusion flux coefficients) closely matches the DNS energy spectrum. This was achieved by suitably selecting the parametric inputs to the model spectrum provided in Pope (2000), as follows:

$$E(\kappa) = C\epsilon^{2/3}\kappa^{-5/3}f_L(\kappa L)f_\eta(\kappa\eta) \quad (4.1)$$

$$f_L(\kappa L) = \left(\frac{\kappa L}{[(\kappa L)^2 + c_L]^{1/2}} \right)^{5/3+p_0} \quad (4.2)$$

$$f_\eta(\kappa\eta) = \exp \left\{ -\beta \left([(\kappa\eta)^4 + c_\eta^4]^{1/4} - c_\eta \right) \right\} \quad (4.3)$$

where $\beta = 5.2$ and $p_0 = 2$ (Pope 2000). The parameters c_L and c_η are determined from the following constraints:

$$\frac{3}{2}u_{\text{rms}}^2 = \int_1^{\kappa_{\text{max}}} E(\kappa) d\kappa \quad (4.4)$$

$$\epsilon = 2\nu \int_1^{\kappa_{\text{max}}} \kappa^2 E(\kappa) d\kappa \quad (4.5)$$

where ϵ is the dissipation rate, and the wavenumber limits $[1, \kappa_{\text{max}}]$ are the same as in DNS. These wavenumber limits are also used in calculating the drift and diffusion flux coefficients. The parameters c_L and c_η are numerically evaluated using the DNS values of u_{rms} , ϵ and ν from Table 2. The resulting values of c_L and c_η are shown in Table 3. In

| Parameter | DNS I |
|---------------------------|----------------------|
| N | 128 |
| Re_λ | 77.756 |
| u_{rms} | 0.968 |
| ν | 0.0071 |
| ϵ | 0.307 |
| L | 1.518 |
| λ | 0.572 |
| η | 0.033 |
| T_E | 1.568 |
| τ_η | 0.153 |
| $\kappa_{\text{max}}\eta$ | 1.991 |
| Δt | 2.5×10^{-3} |
| N_p | 300,000 |

Table 2: Simulation parameters for the DNS study. All dimensional parameters are in arbitrary units. $Re_\lambda \equiv u_{\text{rms}}\lambda/\nu$ is the Taylor micro-scale Reynolds number, $u_{\text{rms}} \equiv \sqrt{(2k/3)}$ is the fluid RMS fluctuating velocity, k is the turbulent kinetic energy, ν is the fluid kinematic viscosity, $\epsilon \equiv 2\nu \int_0^{\kappa_{\text{max}}} \kappa^2 E(\kappa) \, d\kappa$ is the dissipation rate of turbulent kinetic energy, $L \equiv 3\pi/(2k) \int_0^{\kappa_{\text{max}}} E(\kappa)/\kappa \, d\kappa$ is the integral length scale, $\lambda \equiv u_{\text{rms}}\sqrt{(15\nu/\epsilon)}$ is the Taylor microscale, $\eta \equiv \nu^{3/4}/\epsilon^{1/4}$ is the Kolmogorov length scale, $T_E \equiv L/u_{\text{rms}}$ is the large-eddy turnover time, $\tau_\eta \equiv \sqrt{(\nu/\epsilon)}$ is the Kolmogorov time scale, κ_{max} is the maximum resolved wavenumber, Δt is the time step, and N_p is the number of particles per Stokes number.

| Parameter | Value |
|-----------------------|--------|
| C | 1.908 |
| c_L | 0.2855 |
| c_η | 0.2165 |
| κ_{max} | 60 |

Table 3: Parameters for the model energy spectrum at $Re_\lambda = 77.76$. After determining c_L and c_η , the parameter C was adjusted to match the DNS energy spectrum. Pope (2000) suggested $C = 1.5$.

figure 1, the model spectra calculated from equations (4.1)-(4.3) are compared with the DNS energy spectrum for $Re_\lambda = 77.76$. Good agreement is seen between the model and DNS spectra.

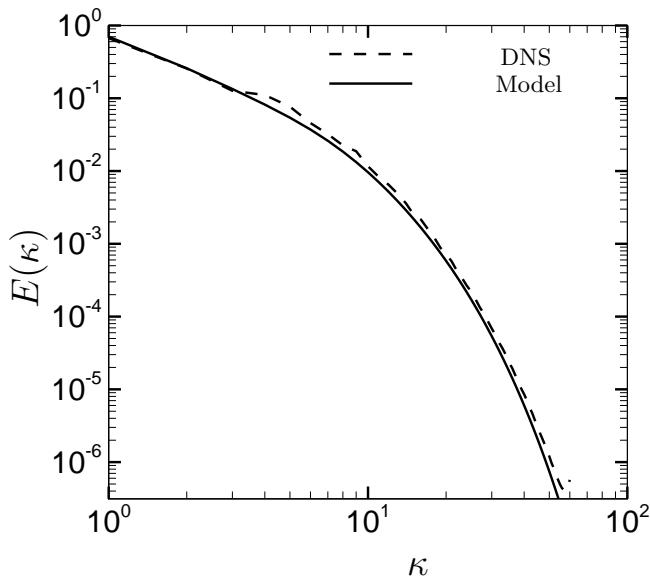


Figure 1: Comparison of the DNS and model energy spectra at $Re_\lambda = 77.76$.

5. Results

We have shown in the Part I paper that the PDF of pair separation is given by

$$\langle P \rangle(r, \mu) = r^{\beta_2 St_\eta^2} \frac{1}{4\pi} \left[1 + St_\eta^2 \beta_2 \left(\frac{1}{2} \ln(1 - \mu^2) - (\ln 2 - 1) \right) \right] \quad (5.1)$$

where $\mu = \cos \theta$, with $\theta \in (-\pi, \pi)$ being the spherical polar angle. The power-law exponent β_2 is given by

$$\beta_2 = \frac{\lambda_2 + 2\lambda_1}{\alpha_2} \quad (5.2)$$

where λ_1 and λ_2 are the drift flux coefficients, and α_2 is the diffusion flux coefficient. These coefficients are determined through a numerical quadrature process, discussed in Part I. It may be recalled that there are two forms of λ_1 and λ_2 , corresponding to the two drift closures DF1 and DF2. Thus, we will compare two theoretical values of β_2 with the corresponding DNS value.

DNS were performed at a Taylor micro-scale Reynolds number $Re_\lambda = 77.76$ for three Froude numbers $Fr = \infty, 0.052, 0.006$, where $Fr = \infty$ corresponds to zero gravity, and $Fr = 0.006$ to the highest magnitude of gravity considered in the current DNS. For each Fr , particles of six Stokes numbers $St_\eta = 0.01, 0.02, 0.04, 0.08, 0.15, 0.2$ were tracked. Spatial clustering of particles is quantified through the radial distribution function (RDF), $g(r)$, which scales with separation r as $g(r) \sim r^{\beta_2 St_\eta^2}$ for $r \ll \eta$. The DNS value of the exponent β_2 is then determined through a least squares curve fit of the RDF for $0.6\eta \leq r \leq 2.5\eta$.

In figure 2, we compare the exponent $(-\beta_2 \times St_\eta^2)$ obtained from DNS and theory. The theoretical β_2 's for both DF1 and DF2 (valid in the $Fr \ll 1$ limit), and the DNS β_2 's for the three Fr 's are presented in figure 2. A key feature of DF2 is that it accounts for the two-time autocorrelations and cross-correlations of dissipation rate

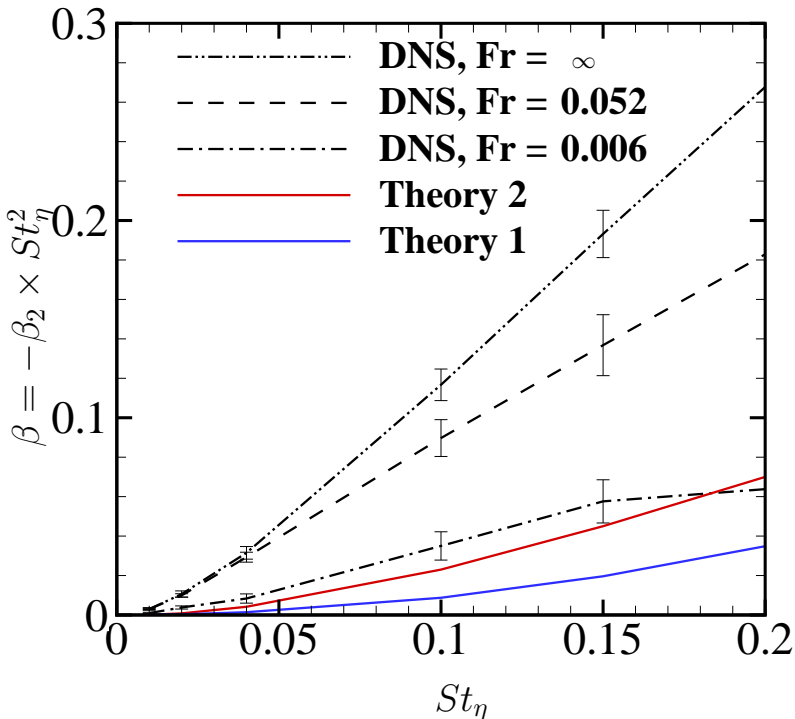


Figure 2: Comparison of the power-law exponent β obtained from theory and DNS. Results obtained using both DF1 and DF2 are shown (referred to as Theory 1 and Theory 2, respectively). There is an uncertainty of $\sim 8\%$ in the DNS values of β .

and enstrophy (or, equivalently of the second invariants of strain-rate and rotation-rate tensors). Chun *et al.* (2005) showed that these correlations quantify, as well as illustrate the mechanisms driving the clustering of non-settling particles. It is evident from figure 2 that the DF1 β_2 's are significantly lower than those of DNS for all three Froude numbers. However, the DF2 β_2 's are in reasonable agreement with the DNS β_2 's for $Fr = 0.006$. The improved performance of DF2, compared to DF1, is because DF2 accounts for the correlations of dissipation rate and enstrophy, but DF1 does not.

Next, we consider the anisotropy in particle clustering due to settling. Ireland *et al.* (2016) quantified the anisotropy through the use of the angular distribution function (ADF), $g(\mathbf{r})$, and expressed it in terms of the Legendre spherical harmonic functions, as below.

$$\frac{g(\mathbf{r})}{g(r)} = \sum_{l=1}^{\infty} \frac{\mathcal{C}_{2l}^0(r)}{\mathcal{C}_0^0(r)} Y_{2l}^0(\cos \theta) \quad (5.3)$$

where

$$g(r) = \mathcal{C}_0^0(r) = \int_0^\pi d\theta \sin \theta g(\mathbf{r}) \quad (5.4)$$

describes the dependence of clustering on separation r . Applying the orthogonality of

| St_η | Theory (DF2) | DNS ($Fr = 0.006$) |
|-----------|-----------------------|-----------------------|
| 0.01 | 4.17×10^{-5} | 3.84×10^{-4} |
| 0.02 | 3.33×10^{-4} | 2.82×10^{-4} |
| 0.04 | 1.73×10^{-3} | 1.42×10^{-3} |
| 0.05 | 2.50×10^{-3} | 2.23×10^{-3} |
| 0.10 | 9.58×10^{-3} | 8.68×10^{-3} |
| 0.15 | 1.88×10^{-2} | 1.12×10^{-2} |
| 0.20 | 2.92×10^{-2} | 1.42×10^{-2} |

Table 4: Comparison of $\mathcal{C}_2^0(r)/\mathcal{C}_0^0(r)$ obtained using theory (DF2 only) and current DNS for $Fr = 0.006$. There is an uncertainty of $\sim 10\%$ in the DNS values of the coefficient ratio.

Legendre polynomials to (5.3), we get

$$\frac{\mathcal{C}_2^0(r)}{\mathcal{C}_0^0(r)} = \frac{5}{2} \frac{\int_0^\pi d\theta \sin \theta g(r) Y_2^0(\cos \theta)}{g(r)} \quad (5.5)$$

The theoretical value of the coefficient ratio is

$$\begin{aligned} \left[\frac{\mathcal{C}_2^0(r)}{\mathcal{C}_0^0(r)} \right]_{\text{theory}} &= \frac{5}{2} \frac{\int_0^\pi d\theta \sin \theta \langle P \rangle(r, \theta) Y_2^0(\cos \theta)}{\int_0^\pi d\theta \sin \theta \langle P \rangle(r, \theta)} \\ &= \frac{5\beta_2 St_\eta^2}{12} \end{aligned} \quad (5.6)$$

In table 4, we compare the values of $\mathcal{C}_2^0(r)/\mathcal{C}_0^0(r)$ obtained using theory and DNS, the latter for $Fr = 0.006$. We see that the degree of anisotropy predicted by the theory is in reasonable agreement with that computed using DNS, particularly for $St_\eta \leq 0.10$. However, the theory generally overpredicts the coefficient ratio as compared to DNS.

6. Conclusions

Part II of this study focuses on the quantitative analysis of the theory through a direct comparison of theory predictions with the data obtained in our DNS runs. While the theory is derived in the $Fr \ll 1$ regime, DNS were performed for three Froude numbers $Fr = \infty, 0.052, 0.006$ at $Re_\lambda = 77.76$. In the DNS runs, the $Fr = 0.006$ case represented the run with the highest magnitude of gravitational acceleration. For this case, a domain size of 4π was used in the direction of gravity to mitigate the numerical errors arising from particles spuriously sampling the same eddies more than once as they settle through the domain. A model energy spectrum was derived that closely matched the DNS energy spectrum. The correlation length scales of dissipation rate and enstrophy, $L_{\epsilon\epsilon}$ and $L_{\zeta\zeta}$, needed for DF2 were also obtained using DNS. The model energy spectrum, and the two correlation lengths were then used in the calculation of the drift and diffusion coefficients needed for the power law exponent, as well as the coefficient ratio (for quantifying anisotropy). In terms of the dependence of clustering on separation, we see that the DF1 β 's are significantly lower than the DNS β 's for the three Froude numbers. But, the DF2 β 's are in reasonable quantitative agreement with

the DNS values for $Fr = 0.006$. We also quantified the anisotropy in particle clustering due to the settling. We see that the values of the coefficient ratio $\mathcal{C}_2^0(r)/\mathcal{C}_0^0(r)$ obtained using DF2 are in reasonable agreement with the DNS values at $Fr = 0.006$, particularly for $St_\eta \leq 0.1$. These results demonstrate that the two-time correlations of dissipation rate and entropy constitute an important mechanism driving the drift flux responsible for clustering. The current two-part study presents the development and analysis of an analytical theory for the clustering of low-inertia particle pairs that are settling rapidly in isotropic turbulence. We see that the theory accurately captures the quantitative trends in particle clustering. It also shows reasonable quantitative agreement with DNS data for low Stokes and Froude numbers.

Acknowledgements

SLR gratefully acknowledges NSF support through the grant CBET-1436100.

REFERENCES

- AYALA, ORLANDO, ROSA, BOGDAN, WANG, LIAN-PING & GRABOWSKI, WOJCIECH W 2008 Effects of turbulence on the geometric collision rate of sedimenting droplets. part 1. results from direct numerical simulation. *New Journal of Physics* **10** (7), 075015.
- BEC, JÉRÉMIE, HOMANN, HOLGER & RAY, SAMRIDDHI SANKAR 2014 Gravity-driven enhancement of heavy particle clustering in turbulent flow. *Physical review letters* **112** (18), 184501.
- BRUCKER, K. A., ISAZA, J. C., VAITHIANATHAN, T. & COLLINS, L. R. 2007 Efficient algorithm for simulating homogeneous turbulent shear flow without remeshing. *J. Comp. Phys.* **225**, 20–32.
- CHUN, JAEHUN, KOCH, DONALD L, RANI, SARMA L, AHLUWALIA, ARUJ & COLLINS, LANCE R 2005 Clustering of aerosol particles in isotropic turbulence. *Journal of Fluid Mechanics* **536**, 219–251.
- DHARIWAL, ROHIT & BRAGG, ANDREW D 2018 Small-scale dynamics of settling, bidisperse particles in turbulence. *Journal of Fluid Mechanics* **839**, 594–620.
- IRELAND, PETER J, BRAGG, ANDREW D & COLLINS, LANCE R 2016 The effect of reynolds number on inertial particle dynamics in isotropic turbulence. part 2. simulations with gravitational effects. *Journal of Fluid Mechanics* **796**, 659–711.
- IRELAND, PETER J, VAITHIANATHAN, T, SUKHESWALLA, PARVEZ S, RAY, BAIDURJA & COLLINS, LANCE R 2013 Highly parallel particle-laden flow solver for turbulence research. *Computers & Fluids* **76**, 170–177.
- ONISHI, RYO, TAKAHASHI, KEIKO & KOMORI, SATORU 2009 Influence of gravity on collisions of monodispersed droplets in homogeneous isotropic turbulence. *Physics of Fluids* **21** (12), 125108.
- PARISHANI, H, AYALA, O, ROSA, B, WANG, L-P & GRABOWSKI, WW 2015 Effects of gravity on the acceleration and pair statistics of inertial particles in homogeneous isotropic turbulence. *Physics of Fluids* **27** (3), 033304.
- POPE, S. B. 2000 *Turbulent Flows*. New York: Cambridge University Press.
- WITKOWSKA, A, JUVÉ, D & BRASSEUR, JG 1997 Numerical study of noise from isotropic turbulence. *Journal of Computational Acoustics* **5** (03), 317–336.
- WOITTIEZ, ERIC JP, JONKER, HARM JJ & PORTELA, LUÍS M 2009 On the combined effects of turbulence and gravity on droplet collisions in clouds: a numerical study. *Journal of the atmospheric sciences* **66** (7), 1926–1943.